NATIONAL ADVISORY COMMITTEE
FOR AERONAUTICS

TECHNICAL NOTE 4355

LOW TIP MACH NUMBER STALL CHARACTERISTICS AND HIGH TIP

MACH NUMBER COMPRESSIBILITY EFFECTS ON A HELICOPTER

ROTOR HAVING AN NACA 0009 TIP AIRFOIL SECTION

By Robert D. Powell, Jr., and Paul J. Carpenter

Langley Aeronautical Laboratory
Langley Field, Va.

Washington

July 1958

NATIONAL ADVISORY COMMITTEE FOR AERONAUTICS

TECHNICAL NOTE 4355

LOW TIP MACH NUMBER STALL CHARACTERISTICS AND HIGH TIP

MACH NUMBER COMPRESSIBILITY EFFECTS ON A HELICOPTER

ROTOR HAVING AN NACA 0009 TIP AIRFOIL SECTION

By Robert D. Powell, Jr., and Paul J. Carpenter

SUMMARY

An investigation has been conducted on the Langley helicopter test tower to determine experimentally the low tip Mach number stall and high tip Mach number drag divergence characteristics of a helicopter rotor having an NACA 0009 tip airfoil section, which tapered to an NACA 0017 root airfoil section and had -5.4° of twist. Data are presented for blade tip Mach numbers M_t of 0.28 to 0.72 with corresponding values of tip Reynolds number of 1.65×10^6 to 4.29×10^6. Comparisons are made of the present rotor with unpublished data on a similar rotor but having NACA 0015 tip airfoil sections. At low tip Mach numbers, the blade maximum mean lift coefficient for the blade having the 9-percent-thick tip airfoil section was about 0.16 less than that obtained with the blade having the 15-percent-thick tip airfoil section. At the highest tip Mach number of 0.72, the blade mean lift coefficient for drag divergence was about 0.42 for the blades having 9-percent-thick tip airfoil sections as compared with 0.22 for similar blades having 15-percent-thick tip airfoil sections.

Low wind velocities of 2 to 12 miles per hour reduced the low tip Mach number (0.28 to 0.32) maximum blade mean lift coefficient by 5 to 7 percent. The average airfoil section lift-curve slope required for predicting rotor thrust varied from 5.8 at a tip Mach number of 0.28 to about 7.0 at a tip Mach number of 0.72. The break (nose down) in the pitching moments was delayed past the Mach number for drag divergence.

The efficiency of the rotor decreased with an increase in tip speed. Expressed as figure of merit, at $M_t = 0.28$ the value was about 0.75, and at $M_t = 0.72$ the maximum value was decreased to about 0.66. Similar measurements made on a rotor having an NACA 0015 tip airfoil section showed a value of 0.58 at $M_t = 0.73$.

INTRODUCTION

One method of meeting the requirements of increased helicopter speeds and higher disk loadings is by increasing the rotor-blade tip speed. Design studies of helicopters with rotor tip speeds in the high subsonic Mach number range and with high blade loadings have emphasized the need for experimental rotor performance and blade pitching-moment data.

This investigation is a continuation of a general research program (refs. 1 to 3) to determine the low-tip-speed stall and high-tip-speed compressibility effects on rotors having various NACA airfoil sections as the primary variable. Although these data are limited to hovering and very low forward speeds, the onset and rate of growth of the stall and compressibility effects can be analyzed to provide guidance in the selection of airfoil sections for high-speed rotors. The present paper extends the program to include a rotor having an NACA 0009 airfoil section at the blade tip. The root airfoil section was an NACA 0017 airfoil section and the rotor blades had -5.4° of twist.

The hovering performance of the rotor over a tip Mach number range of 0.28 to 0.72 is presented. The blade stall and compressibility drag-rise characteristics are discussed and a comparison of the performance of the present rotor with unpublished data on a similar rotor, having 15-percent-thick tip airfoil sections, is presented for selected low and high tip Mach number conditions.

The experimental Mach numbers for drag divergence are also compared with those shown by two-dimensional data. Some data on the effect of low wind velocities on rotor blade maximum mean lift coefficient are also presented.

The rotor blades were tested on the Langley helicopter test tower over a tip Mach number range of 0.28 to 0.72 (disk loadings up to 5.4 pounds per square foot) with a corresponding blade tip Reynolds number range of 1.65×10^6 to 4.29×10^6.

SYMBOLS

a   straight-line slope of section lift coefficient with section angle of attack, c_l/α_r, radian measure (assumed to be 5.73 in calculations for incompressible flow conditions)

$\bar{a}$ experimental mean slope of curve of variation of blade section lift coefficient with section angle of attack (radian measure)

b   number of blades

c   blade chord at radius r, ft

t   maximum blade thickness at radius r, ft

c_e equivalent blade chord, $\dfrac{\displaystyle\int_0^R cr^2dr}{\displaystyle\int_0^R r^2dr}$, ft

r   radial distance to a blade element, ft

R   rotor blade radius, ft

T   rotor thrust, lb

Q   rotor torque, lb-ft

M   rotor blade pitching moment, lb-ft

M_t rotor blade tip Mach number

σ rotor solidity, $bc_e/\pi R$

μ coefficient of viscosity, slugs/ft-sec

ρ mass density of air, slugs/cu ft

N_{Re} Reynolds number at blade tip, $\dfrac{\rho\Omega Rc_t}{\mu}$

Ω rotor angular velocity, radians/sec

α_r blade section angle of attack, deg

θ blade section pitch angle measured from line of zero lift, radians

φ inflow angle at blade element, $\theta - \alpha_r$, radians

c_d airfoil section drag coefficient

$c_{d,o}$ airfoil section profile-drag coefficient

c_l airfoil section lift coefficient

$\bar{c}_l$ mean rotor blade lift coefficient, $6C_T/\sigma$

C_T rotor thrust coefficient, $\dfrac{T}{\pi R^2 \rho (\Omega R)^2}$

C_Q rotor torque coefficient, $\dfrac{Q}{\pi R^2 \rho (\Omega R)^2 R}$

C_M rotor blade pitching-moment coefficient, $\dfrac{M}{\dfrac{R\rho}{2}(\Omega R)^2 c_e^2}$

Q_o rotor profile-drag torque, lb-ft

$C_{Q,o}$ rotor profile-drag torque coefficient, $\dfrac{Q_o}{\pi R^2 \rho (\Omega R)^2 R}$

Subscript:

t   at blade tip

The figure of merit is equal to $0.707 C_T^{3/2}/C_Q$.

APPARATUS AND TEST METHODS

Rotor Blades

The rotor used for this investigation was a fully articulated, two-blade rotor with flapping hinge located on the center line of rotation and the drag hinge 12 inches outboard of the center line. The distance from the ground to the rotor hub center was 42 feet.

A sketch of the rotor blade with pertinent dimensions is shown in figure 1. The rotor blades used in the investigation were constructed of wood and incorporated a steel strap near the leading edge to locate the center of gravity at the 25 percent chord.

The radius of the blade from the center line of rotation was 18.68 feet and the rotor solidity was 0.032. The blade had a root chord of 1.15 feet and tapered linearly to 0.84 foot at the tip. The blade airfoil section at the root was an NACA 0017. The section was tapered to an NACA 0012.2 at the 3/4 radius and to an NACA 0008.8 at the blade tip. The outer 25 percent of the rotor blade was finished to true airfoil contour with tolerances of +0.000 and -0.005 inch and was smooth and fair over the entire chord. The remaining part of the rotor blade deviated from the true airfoil shape somewhat more; however, it was smooth and fair over the entire chord. The rotor blade had 5.4° of nonlinear washout (about 0.28° per foot of twist from the root to about 68-percent blade radius and 0.32° per foot from 0.68R to the tip).

In order to study the low-speed stall characteristics, two rows of tufts were attached to one rotor blade. The first row, consisting of 13 tufts, was attached to the blade $2\frac{1}{2}$ inches from the leading edge beginning at $2\frac{1}{2}$ inches from the tip and spaced at 1-foot intervals. The second row was attached 7 inches behind the leading edge and then staggered $1\frac{1}{4}$ inches inboard behind the first row. The tufts were black nylon yarn about 3 inches long. A high-speed motion-picture camera was mounted on the rotor head to record the tuft patterns.

Test Methods and Accuracy

The tests were run by setting given rotor-blade collective pitch angles and varying the rotor speed through a range of tip Mach numbers until either the blade limiting stress was reached or until a further increase in blade pitch did not increase the rotor thrust. At each pitch setting, data were recorded from visual dial readings and by an oscillograph. Quantities measured were rotor thrust, rotor torque, blade pitch angle, blade pitching moment, rotor shaft rotational speed, blade drag angle, and blade flapping angle. The range of test conditions was chosen to determine the low-tip-speed rotor maximum blade mean lift coefficients and the high-tip-speed compressibility drag rise. In addition, tests were made at various low wind speeds (2 to 12 miles per hour) to determine their effect on the rotor maximum mean lift coefficient.

The estimated accuracies of the basic quantities measured during the test are as follows:

Rotor thrust, lb . . . . ±20
Rotor torque, lb-ft . . . . ±50
Rotor rotational speed, rpm . . . . ±1
All angular measurements, deg . . . . ±0.2

The overall accuracy of the plotted results is believed to be within
±3 percent. For example, at a rotor blade mean lift coefficient $\bar{c}_l$
of 0.38 $\left(C_T = 0.00203\right)$ and an $M_t = 0.60$, the accuracy of the plotted
data based on repeatability was about 2 percent for the thrust value of
2,497 pounds, 2 percent for the torque value of 2,145 pound-feet, and
0.3 percent for a rotational-speed value of 342 revolutions per minute.

METHOD OF ANALYSIS

Tests of references 1 to 3 have shown that the principal effect of
compressibility has been a rapid increase in profile-drag torque once
the critical combination of tip speed and tip angle of attack has been
exceeded.

A convenient reference for the rate of growth of profile torque
losses is the ratio of the profile-drag torque coefficient deduced from
the test results to that calculated by using conventional strip analysis
(ref. 4) and incompressible drag coefficients. The calculated rotor-
performance curve is based on a linear lift-coefficient slope ($c_l = a\alpha_r$
where $a = 5.73$) and the conventional drag polar $\left(c_{d,o} = 0.0087 - 0.0216\alpha_r + 0.400\alpha_r^2\right)$. Since reference 4 does not allow for any tip loss,
a 3-percent tip-loss factor (outer 3 percent of the blade produces no
lift but has profile drag) was used in the calculations.

Pitching-moment coefficients deduced from the force measured in the
rotor-blade pitch-control linkage are presented in this paper. The coef-
ficients thus include the contribution of both aerodynamic and mass
forces. In this respect, it should be noted that the presence or absence
of abrupt changes in the pitching-moment coefficient is of more signifi-
cance than the actual values.

RESULTS AND DISCUSSION

The effects of compressibility and stall as analyzed from the basic
curves of hovering performance and rotor-blade pitching moments are
presented first.

Rotor Hovering Performance

The low tip Mach number maximum rotor thrust coefficients and high tip Mach number effects of compressibility are shown in figure 2, as the variation of thrust and torque coefficients for blade-tip Mach numbers from 0.28 to 0.72. An incompressible rotor-performance curve calculated by using the method previously discussed is plotted for comparison with the experimental data.

The initial tests indicated a substantial effect of low wind speeds on rotor maximum thrust. Accordingly, data are presented for wind velocities of 0 to 12 miles per hour in figures 2(a) and 2(b).

Zero wind velocity.- The experimental curve at $M_t = 0.28$ for the hovering (zero wind velocity) condition shows good agreement with the calculated curve up to rotor thrust coefficients of about 0.0042 ($\bar{c}_l = 0.79$). Past that point, the experimental data show a large torque increase for a given C_T as the blade approaches maximum lift. The maximum value of $\bar{c}_l$ obtained was 0.995 which, as expected, is substantially less than that obtained with rotors having essentially similar smooth and fair surfaces but constructed with thicker (12 to 15 percent) airfoil sections. For example, the low-speed maximum mean lift coefficient obtained with blades having NACA 0015 tip airfoil sections was 1.15 and 1.13 was measured for blades having 0012 airfoil sections.

Effect of wind velocity on rotor-blade maximum mean lift coefficient.- Previous to these tests, it was thought that the principal effect of wind velocity on rotor performance was a reduction in rotor-induced torque. A procedure to adjust the torque values to that which would have been obtained at zero wind velocity had been devised (ref. 5). This procedure has been found to be valid for ratios of wind velocity to average rotor induced velocity (V/u) of less than 1.0 but overestimates the correction at higher ratios. The magnitude of the overcorrection in the data obtained at 6 to 12 miles per hour is shown in figures 2(a) and 2(b). Velocity ratios V/u ranged from 0.6 to ∞ for these cases. The present tests, however, show that, above the normal range of test conditions (above blade $\bar{c}_l$ of 0.8), wind velocity has a relatively large additional effect of reducing the rotor-blade maximum mean lift coefficient. Figure 2(a) shows these effects for a tip Mach number of 0.28. Above a rotor thrust coefficient of 0.0042 ($\bar{c}_l = 0.79$), reductions in rotor maximum lift of about 5 percent due to wind velocities of 2 to 12 miles per hour were obtained. These results clearly indicate that the maximum mean lift coefficient of the test rotor will not attain true peak values unless the tests are conducted at zero wind velocity. Further tests of rotors having thicker (12 to 18 percent) airfoils show that the effect of wind velocity

on rotor maximum lift decreases as the airfoil thickness increases. Tests of rotors having 18-percent-thick airfoil sections show no effect of wind velocity on rotor maximum lift.

It is probable that this reduction in $\bar{c}_l$ is primarily due to the nonuniform inflow and flapping motion causing the blade section angle of attack to oscillate below and above the stall angle. An oscillatory stall that occurs once per revolution was indicated by the tufts mounted on the blade. An oscillatory section angle of attack would reduce the mean blade lift. Lift hysteresis effects may also be present which would also reduce the rotor lift. The meaning of lift hysteresis is illustrated in the following sketch:
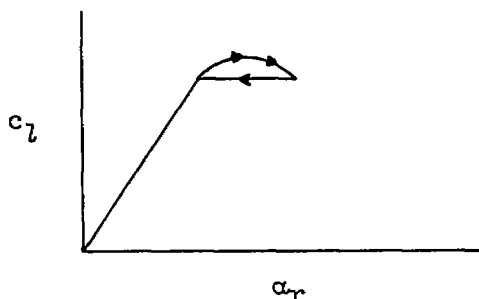
The arrows indicate the path which the lift coefficient follows during the one-per-revolution pitch oscillation. As pitch increases, lift coefficient increases to a maximum value and then falls off owing to flow separation. As pitch decreases, the lift coefficient instead of retracing its previous path remains fairly constant until the point at which the flow reattaches to the airfoil is reached.

Similar reductions in blade maximum lift coefficients were observed as the tip Mach number was increased to 0.32 (fig. 2(b)); however, at the higher tip Mach numbers of 0.36 and 0.41, the effects were found to be negligible.

Effect of compressibility on rotor performance.- Figure 2(c) shows the effect of increasing M_t on rotor hovering performance for the tip Mach number range of 0.36 to 0.72. Torque coefficients have been corrected where data were obtained at wind velocities greater than 5 miles per hour. Figure 2(c) shows that an increase in tip Mach number gives progressively lower values of thrust coefficient for the point where compressibility losses begin. At a tip Mach number of 0.72 and a $\bar{c}_l$ value of 0.6 $\left(C_T = 0.0032\right)$, the rotor blades show a 22-percent increase in the total power due to compressibility losses. It might also be noted

that the zero-lift drag value at M_t ranging from 0.36 to 0.72 was about 10 percent less than the value obtained at M_t = 0.28 or 0.32. This effect was probably due to the beneficial effects of higher Reynolds numbers.

Figure 3 shows a comparison of the characteristics of a low and a high tip Mach number (0.41 and 0.72) of the test rotor with the NACA 0009 airfoil tip section with unpublished data obtained on a rotor having an NACA 0015 airfoil tip section. The two rotors had the same radius, twist, plan-form taper ratio, solidity, surface condition, and nearly identical test conditions. The blades differed principally in airfoil thickness ratio.

Although the data of figure 3 have been obtained on hovering rotors, such results can be used to give an indication of the relative suscepti- bility of the rotors to the stall and compressibility effects associated with forward flight. As an indication of the way in which the high-speed forward-flight stall and compressibility effects on these two rotors might be expected to differ, consider a forward-flight condition in which the advancing blade tip is at M_t = 0.72. These conditions correspond to a rotational tip Mach number of 0.57 and a tip-speed ratio of 0.29.

At the lower tip Mach number of 0.41 corresponding to the assumed tip Mach number of the retreating blade, the data show that the 9-percent- thick blade tip encounters a drag rise at a lower lift coefficient (start of separated flow at tip section) and has a much lower maximum mean lift coefficient than that obtained with the rotor having the 15-percent- thick airfoil section.

At a tip Mach number of 0.72, corresponding to the advancing blade tip for the case assumed, the NACA 0009 airfoil showed a definite supe- riority over the NACA 0015 airfoil by delaying the compressibility drag rise. The 9-percent-thick blade achieved a mean lift coefficient of 0.42 before diverging from the essentially incompressible results (M_t = 0.41) compared with 0.22 for the 15-percent-thick blade. The rate of increase of the rotor torque coefficient, however, is greater for the 9-percent- than for the 15-percent-thick section and eventually the two rotors show similar power requirements as evidenced by the con- vergence of the performance curves.

The results shown by the tests of these two rotors are typical of the results obtained from two-dimensional tests of thin and thick air- foils. The application of these results to predict the overall improve- ment in forward-flight performance that could be obtained with the 9-percent-thick blades is largely dependent on the amount of retreating blade stall that can be tolerated. Inasmuch as the blade-tip angle of

attack is dependent on rotational tip speed, twist, solidity, forward speed, fuselage drag, and the mission requirements, the helicopter would have to be examined in detail to determine the differences in performance with 9- or 15-percent-thick tip airfoil sections.

Low-speed stall flow patterns.- Figure 4 presents the beginning and progression of separated flow as indicated by tuft patterns as blade pitch was increased. An accompanying plot of calculated blade angle of attack along the blade span is also presented for each test condition. The blade thickness distribution is also shown for purposes of correlating stall with airfoil thickness ratio.

Figure 4(b) shows the beginning of separated flow at angles of attack of about 10.25° on that portion of the blade having airfoil thicknesses of 9 and 10 percent. This appeared to be a very sudden leading-edge stall with separated flow over the rest of the airfoil. As would be expected the thicker inboard sections showed no separated flow even though they are at slightly higher calculated angles of attack; this condition can be attributed to the stall delay provided by larger leading-edge radius. These effects of increased low-speed stall angle as leading-edge radius is increased have been well-documented in two-dimensional tests. (See refs. 6, 7, and 8.)

As the blade pitch angle was further increased (fig. 4(c)), additional separated flow at the trailing edge of that part of the blade having 12- to 15-percent-thick airfoils appeared. The separated flow for these thicker sections started at an angle of attack of about 11.2° (1° greater than that for the 9-percent-thick section). The angle of attack for stall of the 12- to 15-percent-thick sections seems to be slightly low in that similar unpublished results of a blade having NACA 0012 airfoil sections showed angles of attack of 12° to 13° before separated flow occurred. It is interesting to note that there was no indication of separated flow at the blade tip, probably because of the downwash from the tip vortex.

Rotor efficiency.- The efficiency of the rotor at various tip Mach numbers, expressed in terms of figure of merit, is shown in figure 5. The maximum figure of merit obtained at the low tip speeds was about 0.75 compared with a value of 0.74 obtained for the 15-percent-thick blades. As the tip Mach number was increased, the maximum figure of merit of the rotor decreased because of the compressibility drag rise. At a tip Mach number of 0.72 the maximum figure of merit dropped to about 0.66 for the rotor under discussion as compared with 0.58 for the rotor with an NACA 0015 airfoil tip section at $M_t = 0.73$.

Effect of tip Mach number on blade lift.- Figure 6 shows the variation in thrust coefficient with changes in blade tip Mach number

$(M_t = 0.28$ to $0.72)$ as a function of the blade pitch angle. As tip Mach number was increased past 0.60, as would be expected, a substantial increase in rotor thrust coefficient for given blade pitch angles was obtained.

Mean blade lift-curve-slope values were deduced from figure 6 for the various tip Mach numbers and are shown in figure 7 as a plot of the ratio of rotor blade mean section-lift-curve slope as a function of blade-tip Mach number. Curves are shown for blade pitch angles at the 3/4 radius for 8° and 12°. The figure shows that the mean lift-curve slope had an average value of 5.8 at tip Mach numbers ranging from 0.28 to about 0.55. As tip Mach number is increased, higher lift-curve-slope values are obtained. For example, at $M_t = 0.72$ a value of $\bar{a}$ equal to about 7.0 would be required to predict the rotor thrust.

Rotor-Blade Pitching Moments

Rotor-blade pitching-moment data are necessary to determine the rotor control forces and are important in blade vibration and stability analysis. A comparison of the blade pitching-moment characteristics for representative tip Mach numbers of 0.28 to 0.72 for the rotor blade tested as a function of rotor thrust coefficient is shown in figure 8. The pitching-moment data represent the measured rotor-blade moments about the blade pitch axis and include aerodynamic and blade mass forces.

Changes in blade pitching-moment coefficient as thrust coefficient is increased are probably largely due to the chordwise displacement of the blade center of pressure from the blade center of gravity. Since the position of the blade center of pressure is not precisely known and since the actual blade pitching moments were reasonably small (3 to 75 pound-feet) no attempt was made to separate the mass moments from the aerodynamic moments. The most important factor is the presence or absence of abrupt changes in pitching-moment slopes rather than the actual values.

The pitching moments throughout the operating range were slightly positive, that is, nose up. There was very little variation in pitching moments with increases in thrust coefficient until the blade approached its maximum thrust coefficient and a portion of the blade stalled. As would be expected, the stall caused a rearward shift of the center of pressure tending to decrease the nose-up pitching moment. The point at which stall or compressibility begins to increase the rotor profile power is noted on figure 8. The reversal in slope (nose-down moment) of the blade pitching-moment characteristic was delayed beyond the onset of drag divergence. This effect has also been noted in two-dimensional tests (ref. 9) as well as in other rotor tests (ref. 2).

Rotor Profile-Drag Torque

The principal effect of compressibility and stall on the rotor performance has been shown to be a rapid increase in the rotor profile-drag torque. (See refs. 1 to 3.)

Figure 9 represents the rate of growth of profile-drag torque as a function of the ratio of $C_{Q,o(\text{measured})}$ to $C_{Q,o(\text{calculated})}$ plotted against rotor blade tip angle of attack. At tip Mach numbers ranging from 0.28 to 0.50, the ratio of profile-drag torque coefficients did not exceed unity up to a calculated blade tip angle of about 7°. This result indicates that there was no drag increase over that represented by the conventional drag polar. In fact, at some of the lower angles, the blade has less profile drag than that shown by the conventional drag polar, as indicated by the data points below a profile torque ratio of unity. Above blade tip angles of 7°, the profile-drag torque coefficient ratios began to diverge from unity and indicated that the conventional drag polar underestimated the actual profile-drag torque. As previously discussed, the flow separation near the tip of the blade occurs at a tip angle of attack of about 10° at the low Mach numbers. This separation results in a steepening of the profile-drag torque curve in this angle-of-attack region. In the low tip Mach number range of 0.28 to 0.50 there is no orderly progression of the tip angle for profile-drag increase as a function of M_t; however, if the results are based on $\bar{c}_l$, they follow established trends which are shown in figure 10.

At Mach numbers beyond 0.5, the principal factor influencing the point of drag rise is the tip Mach number. In general, the curves show that the profile-drag torque was approximately doubled for tip angles of attack 2° beyond the initial drag-rise point.

Figure 10 shows the rotor profile-drag rise as a function of rotor-blade mean lift coefficient. At the low tip Mach numbers (0.28, 0.32), the maximum mean lift coefficient before drag rise was about 0.82. This value of $\bar{c}_l$ is about 8 percent lower than that obtained with a rotor having an NACA 0012 airfoil and about 15 percent lower than that obtained with a rotor having an NACA 0015 airfoil tip. As the tip Mach number was increased, the values of $\bar{c}_l$ for drag rise became more comparable to the thicker sections. For example, at $M_t = 0.50$ the $\bar{c}_l$ drag-rise values were 0.67 for the NACA 0009 tip airfoil section as compared with 0.70 for the NACA 0012 airfoil section and 0.80 for the NACA 0015 airfoil tip section.

At higher tip Mach numbers ($M_t = 0.72$) the 9-percent-thick blade had almost twice as large a lift coefficient for drag divergence as the

similar 15-percent-thick blade. This trend, as tip Mach number is increased, would be expected to continue and show an ever-increasing superiority of the 9-percent- over the 15-percent-thick airfoils.

Comparison With Two-Dimensional Drag-Divergence Data

A comparison of the rotor drag-divergence Mach numbers with those predicted from two-dimensional airfoil data is presented in figure 11. The measured data were obtained from figure 9 and were taken as the point at which the profile-torque coefficient ratio departs from a value of unity. Two-dimensional airfoil data for the NACA 0009-64 and an interpolated curve for the NACA 64-009 (obtained from unpublished NACA 64-008 and NACA 64-010 data) are presented. Two methods of obtaining drag-divergence points are shown: (1) the point at which $\Delta c_d / \Delta M = 0.1$ and (2) the point at which the drag coefficient first begins to increase. The latter is more consistent with the method by which the experimental rotor data were obtained.

It should be noted that, at low tip angles of attack, this rotor blade showed no tip-relief effect, that is, the rotor drag-increase Mach number agrees with the drag-increase Mach number of the two-dimensional data. This result differs from results obtained with other rotors (refs. 1 to 3), which have shown that the point for rotor drag increase is sometimes as much as 0.1 in Mach number greater than that shown by two-dimensional tests. It was expected that this 9-percent-thick blade would also follow in the same general pattern. One possible explanation is dynamic twist of the blade at the higher tip Mach numbers. Calculations for $M_t = 0.7$, if the blade pitching moment is assumed to be distributed along the blade proportional to r^2, indicate that actual blade angle of attack would be 0.5° greater than that shown. At the lower tip Mach numbers, dynamic twist appears to be negligible.

At the higher angles of attack the characteristics of this rotor followed the general trend shown by other rotors, that is, drag-increase Mach numbers lie between the 2 two-dimensional curves.

CONCLUSIONS

The low tip Mach number maximum mean lift coefficients and high tip Mach number compressibility effects on a rotor having an NACA 0009 airfoil tip section, an NACA 0017 airfoil root section, and 5.4° of negative twist have been determined over a tip Mach number (M_t) range of 0.28 to 0.72. As a result of this investigation the following conclusions can be drawn:

1. At low tip Mach numbers, the blade maximum mean lift coefficient was approximately 0.16 lower than that obtained with similar blades having 15-percent-thick tip airfoil sections.

2. At the higher tip Mach numbers experimental data for the 9-percent-thick blade indicated higher values for the mean rotor blade lift coefficient $\bar{c}_l$ at drag divergence than those obtained from tests of a 15-percent-thick blade. At $M_t = 0.72$ the 9-percent-thick tip rotor blade diverged at $\bar{c}_l = 0.42$ compared with a $\bar{c}_l$ value of 0.22 for the 15-percent-thick tip rotor blade.

3. At wind speeds of 2 to 12 miles per hour and at low tip Mach numbers, the maximum rotor mean lift coefficients were reduced from 5 to 7 percent from the values measured at zero wind speed.

4. The mean values of airfoil-section lift-curve slope required for an analytical prediction of the rotor thrust varied from an average value of 5.8 at $M_t = 0.28$ to a value of 7.0 at $M_t = 0.72$.

5. The break (nose down) in the pitching-moment curves was delayed past the Mach number for drag divergence.

6. The 9-percent-thick blade showed very little tip-relief effect for drag divergence at the higher Mach numbers tested when compared with the two-dimensional data.

7. The efficiency of the rotor, expressed as figure of merit, decreased with an increase in tip Mach number. At $M_t = 0.28$ the maximum figure of merit was about 0.75. At $M_t = 0.72$, the maximum figure of merit dropped to 0.66. Similar measurements made on a rotor having an NACA 0015 tip airfoil section showed a value of 0.58 at $M_t = 0.73$.

Langley Aeronautical Laboratory,
    National Advisory Committee for Aeronautics,
        Langley Field, Va., March 21, 1958.

REFERENCES

1. Carpenter, Paul J.: Effects of Compressibility on the Performance of Two Full-Scale Helicopter Rotors. NACA Rep. 1078, 1952. (Supersedes NACA TN 2277.)

2. Shivers, James P., and Carpenter, Paul J.: Experimental Investigation on the Langley Helicopter Test Tower of Compressibility Effects on a Rotor Having NACA 63_2-015 Airfoil Sections. NACA TN 3850, 1956.

3. Powell, Robert D., Jr.: Compressibility Effects on a Hovering Helicopter Rotor Having an NACA 0018 Root Airfoil Tapering to an NACA 0012 Tip Airfoil. NACA RM L57F26, 1957.

4. Gessow, Alfred: Effect of Rotor-Blade Twist and Plan-Form Taper on Helicopter Hovering Performance. NACA TN 1542, 1948.

5. Carpenter, Paul J.: Effect of Wind Velocity on Performance of Helicopter Rotors As Investigated With the Langley Helicopter Apparatus. NACA TN 1698, 1948.

6. Kelly, John A.: Effect of Modifications to the Leading-Edge Region on the Stalling Characteristics of the NACA 63_1-012 Airfoil Section. NACA TN 2228, 1950.

7. Loftin, Laurence K., Jr., and Von Doenhoff, Albert E.: Exploratory Investigation at High and Low Subsonic Mach Numbers of Two Experimental 6-Percent-Thick Airfoil Sections Designed To Have High Maximum Lift Coefficients. NACA RM L51F06, 1951.

8. Gault, Donald E.: A Correlation of Low-Speed, Airfoil-Section Stalling Characteristics With Reynolds Number and Airfoil Geometry. NACA TN 3963, 1957.

9. Wilson, Homer B., Jr., and Horton, Elmer A.: Aerodynamic Characteristics at High and Low Subsonic Mach Numbers of Four NACA 6-Series Airfoil Sections at Angles of Attack From -2° to 31°. NACA RM L53C20, 1953.
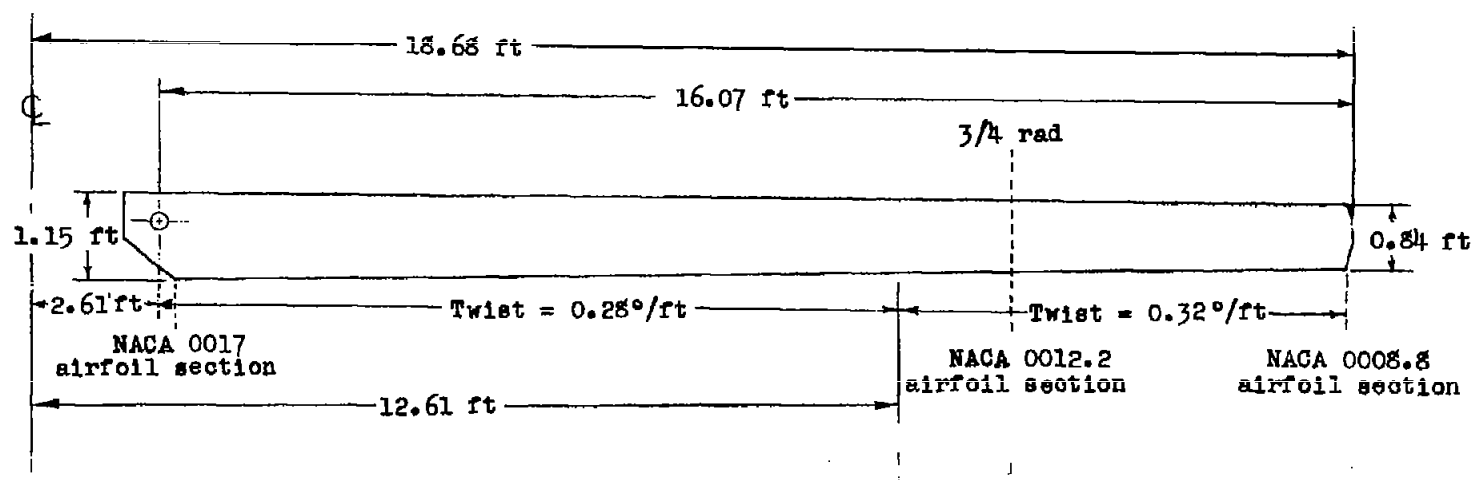
Figure 1.- Sketch of rotor blade having an NACA 0009 airfoil tip section. $c_e = 0.94$ foot.
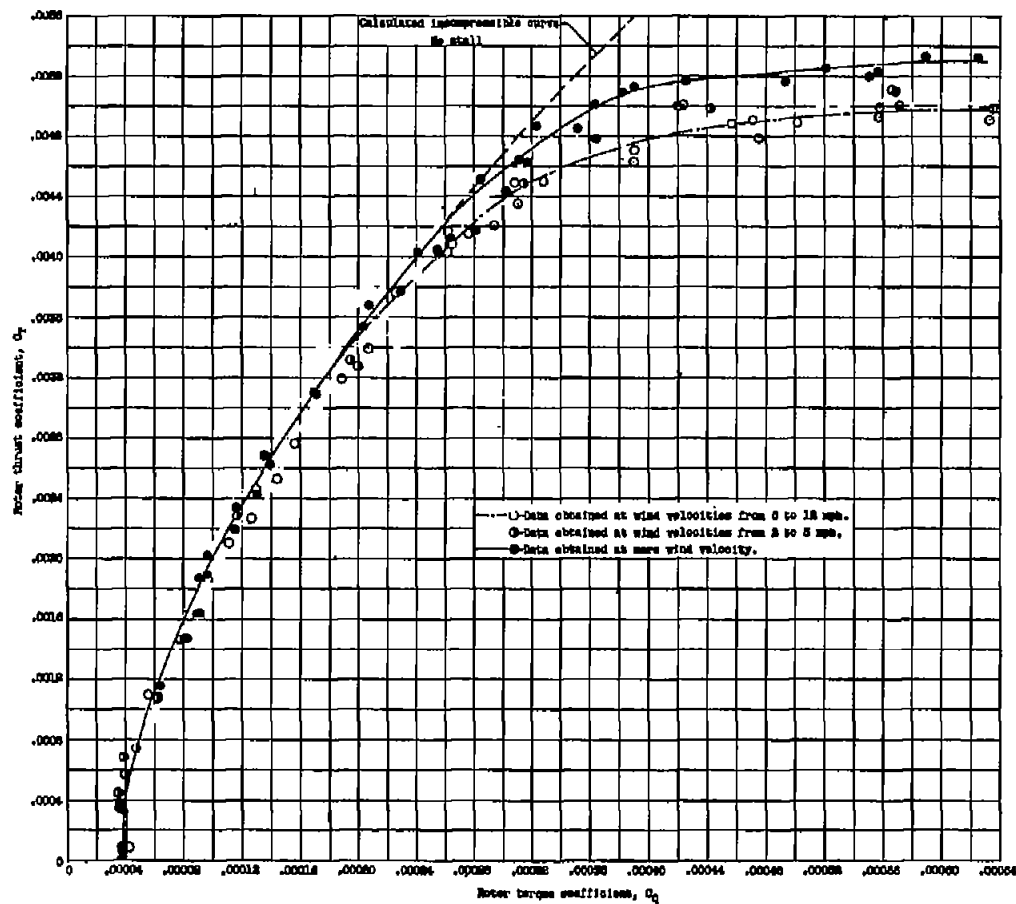
(a) $M_t = 0.28$; $N_{Re} = 1.66 \times 10^6$.

Figure 2.- Hovering performance of rotor blades having NACA 0009 airfoil tip sections. A correction for wind velocity has been applied to the induced torque. Calculated curve based on $c_{d,o} = 0.0087 - 0.0216\alpha_r + 0.400\alpha_r^2$ and $c_l = a\alpha_r$. $\sigma = 0.032$.
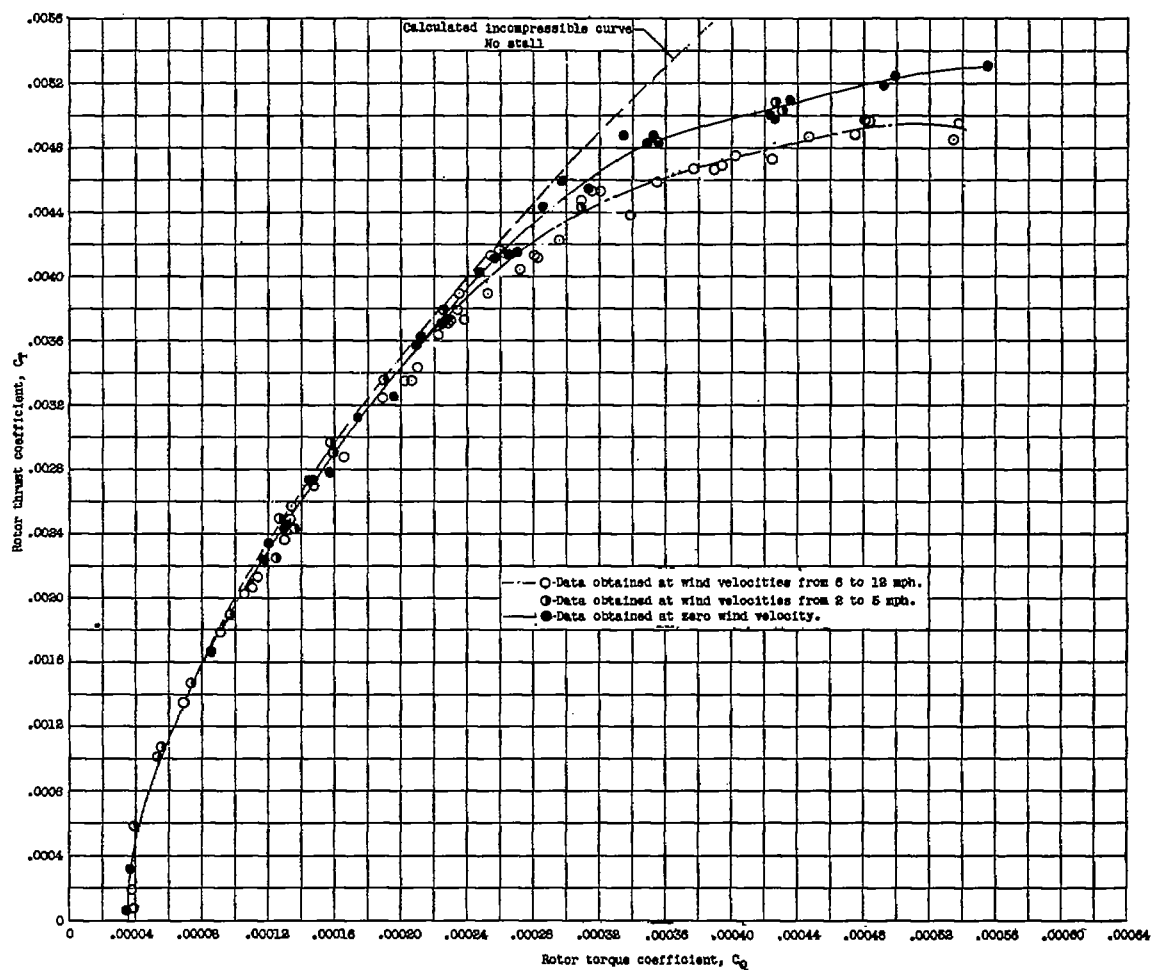
(b) $M_t = 0.32$; $N_{Re} = 1.90 \times 10^6$.

Figure 2.- Continued.
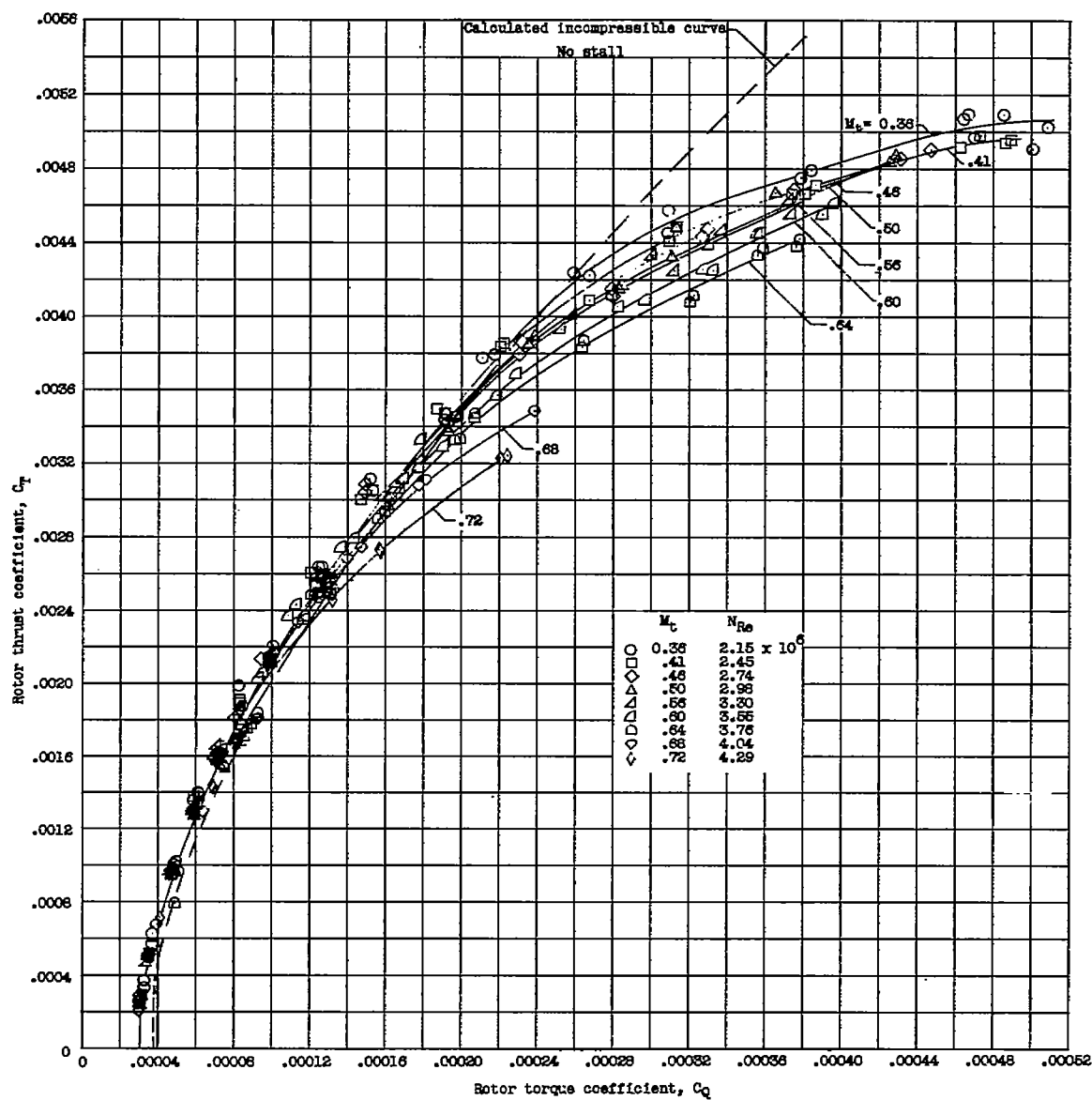
(c) $M_t = 0.36$ to 0.72.

Figure 2.- Concluded.
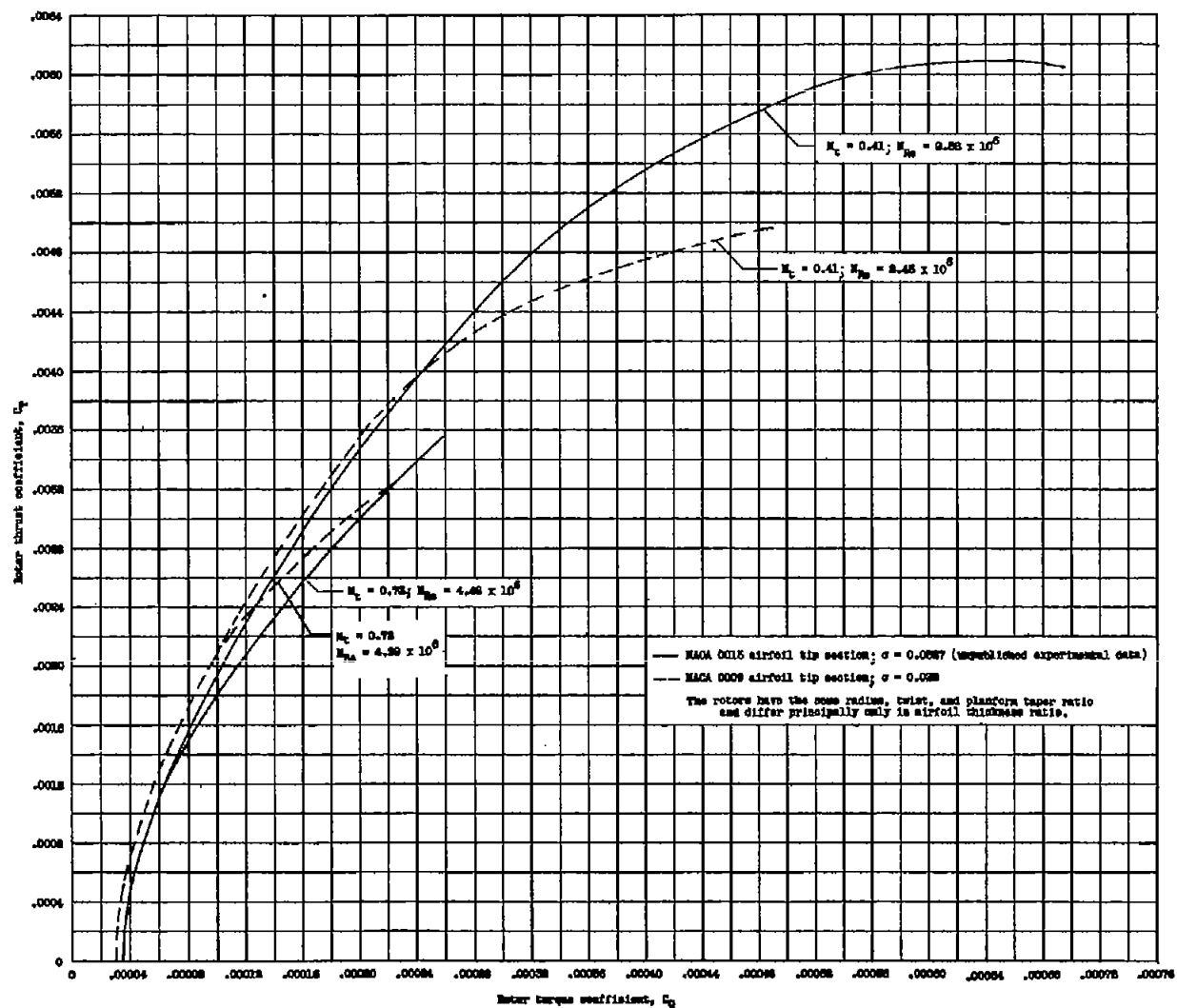
Figure 3.- Effect of airfoil thickness ratio on low and high tip Mach number rotor characteristics.
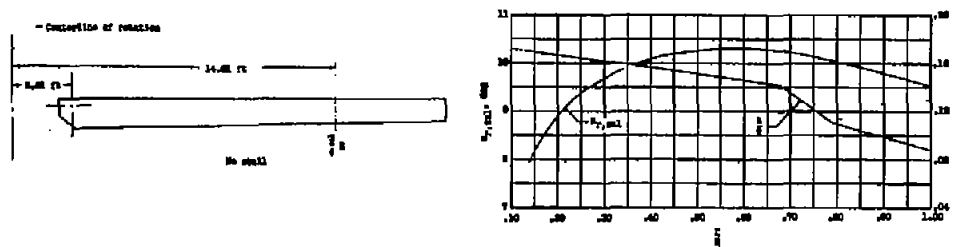
(a) $\alpha_{r,t} = 9.5^\circ$; $\bar{c}_l = 0.96$.
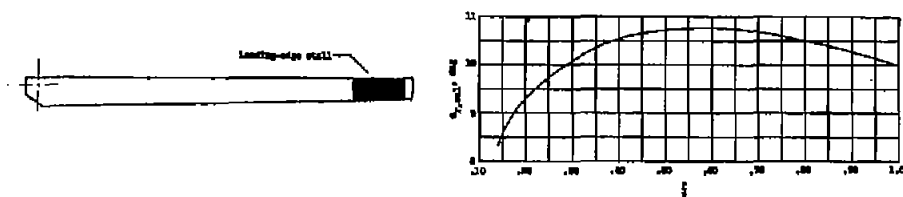
(b) $\alpha_{r,t} = 10.0^\circ$; $\bar{c}_l = 0.98$.
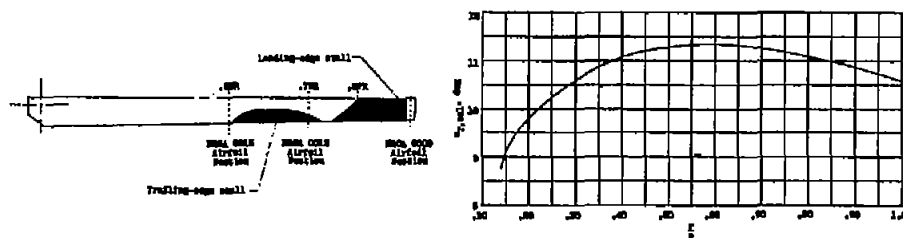
(c) $\alpha_{r,t} = 10.6^\circ$; $\bar{c}_l = 0.99$.

Figure 4.- Sketches of rotor blade at three tip angle-of-attack positions showing the progression of stall as indicated by tuft patterns, and plots of the variation of calculated angle of attack with percent radius. $M_t = 0.32$; $N_{Re} = 1.90 \times 10^6$.
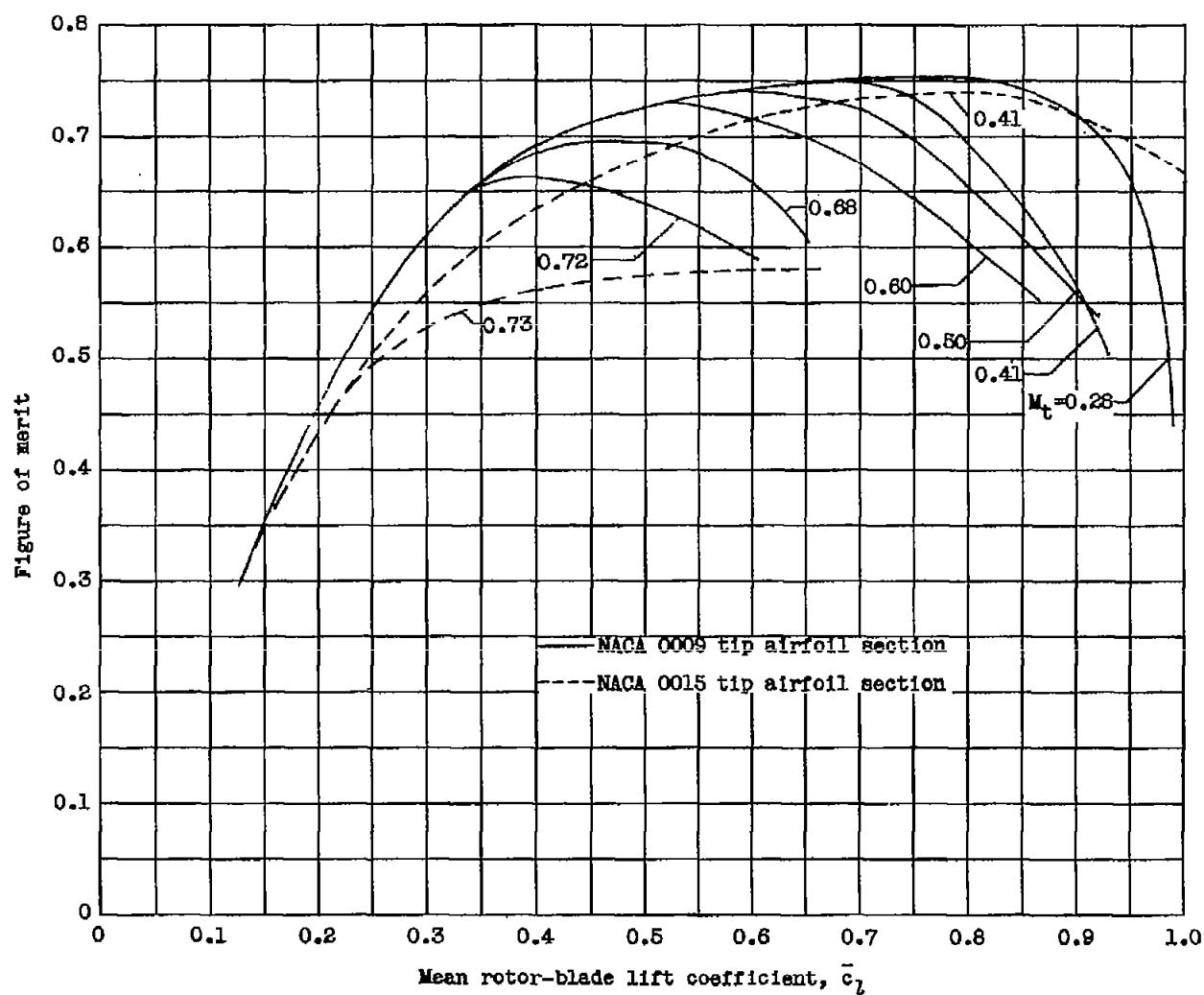
Figure 5.- Effect of tip Mach number on rotor figure of merit $\left(0.707 C_T{}^{3/2}/C_Q\right)$.
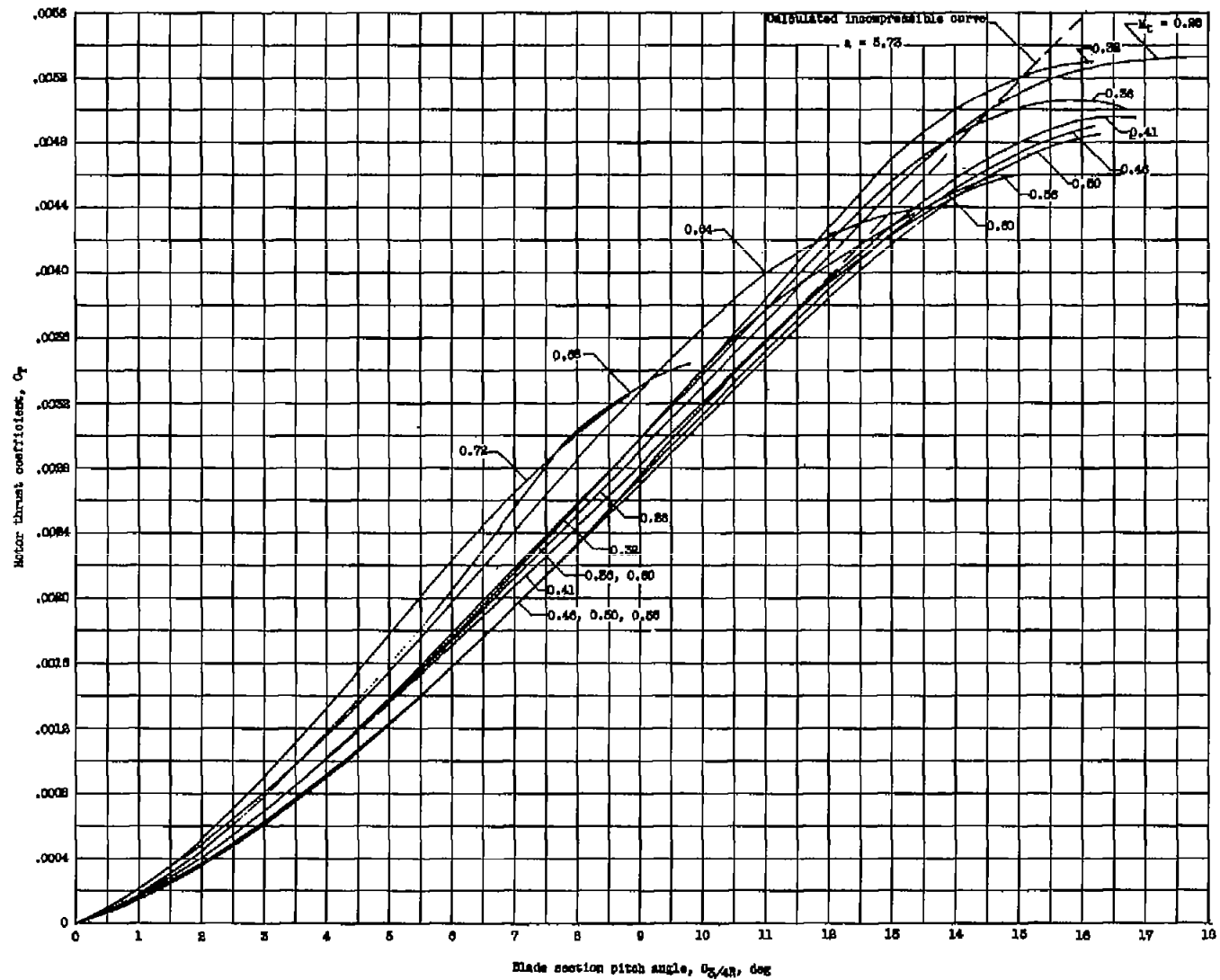
Figure 6.- Effect of tip Mach number on rotor thrust coefficient.
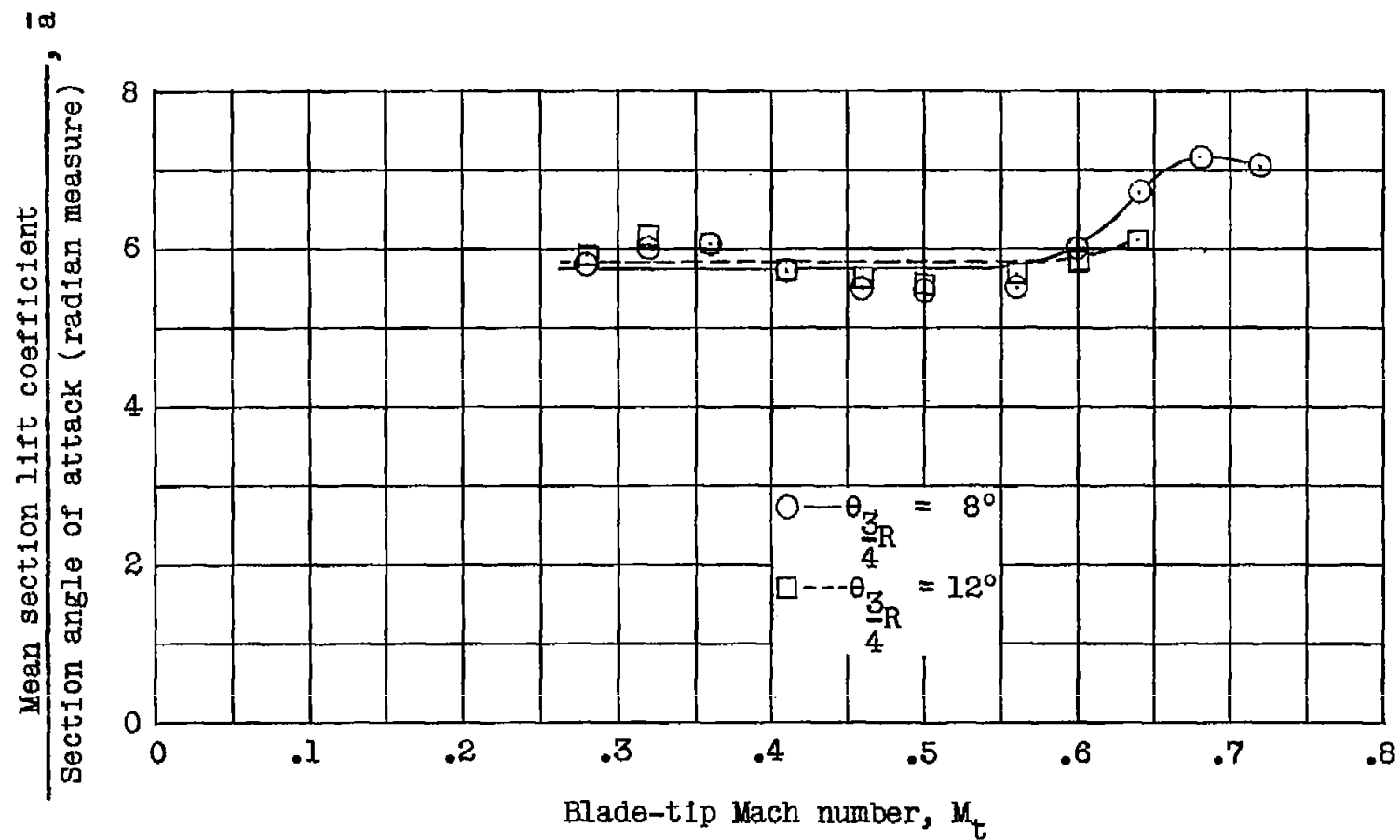
Figure 7.- Airfoil section lift-curve slope required for predicting rotor thrust at various Mach numbers.
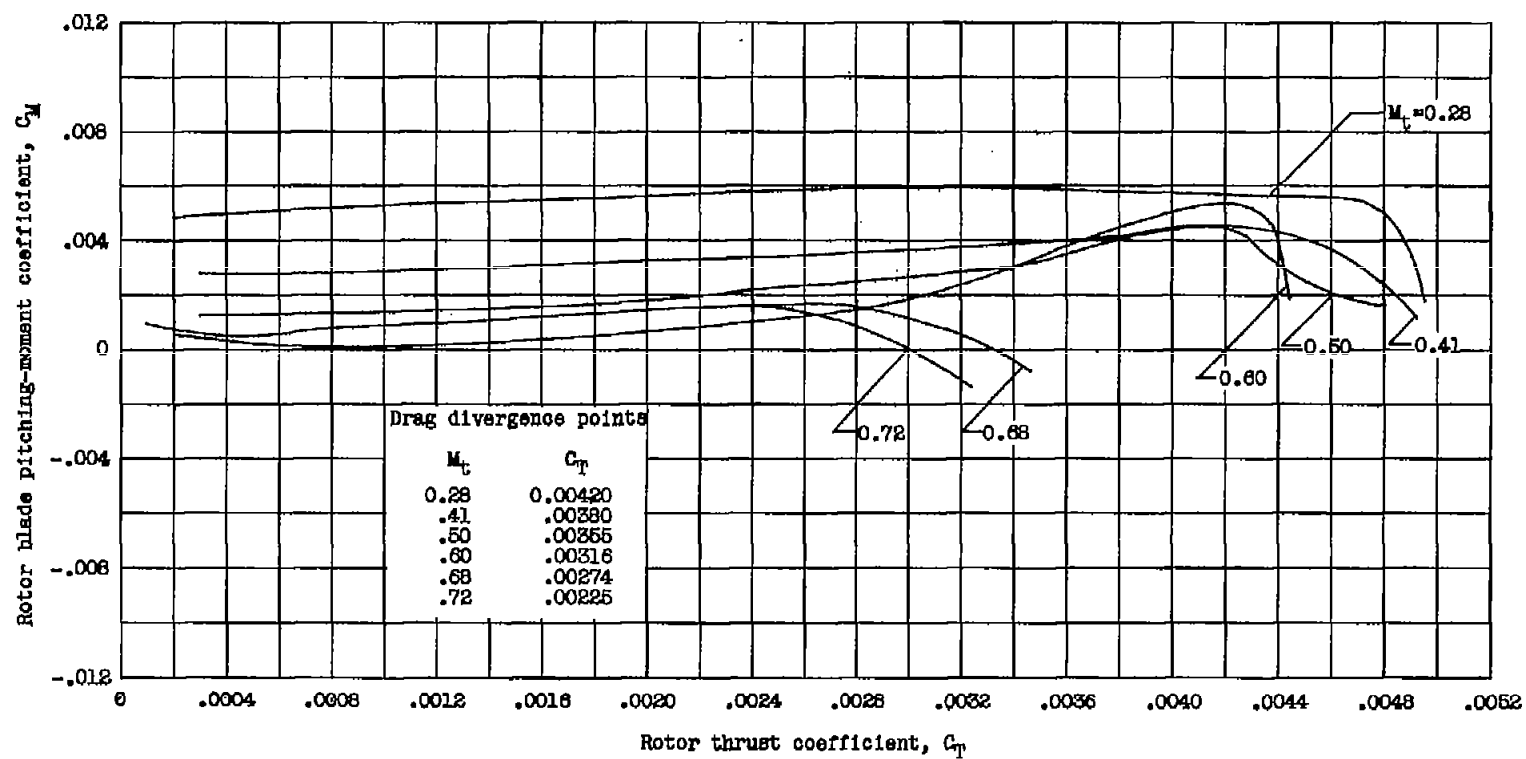
Figure 8.- Effect of tip Mach number on the pitching moments of rotor blades having NACA 0009 tip airfoil sections.
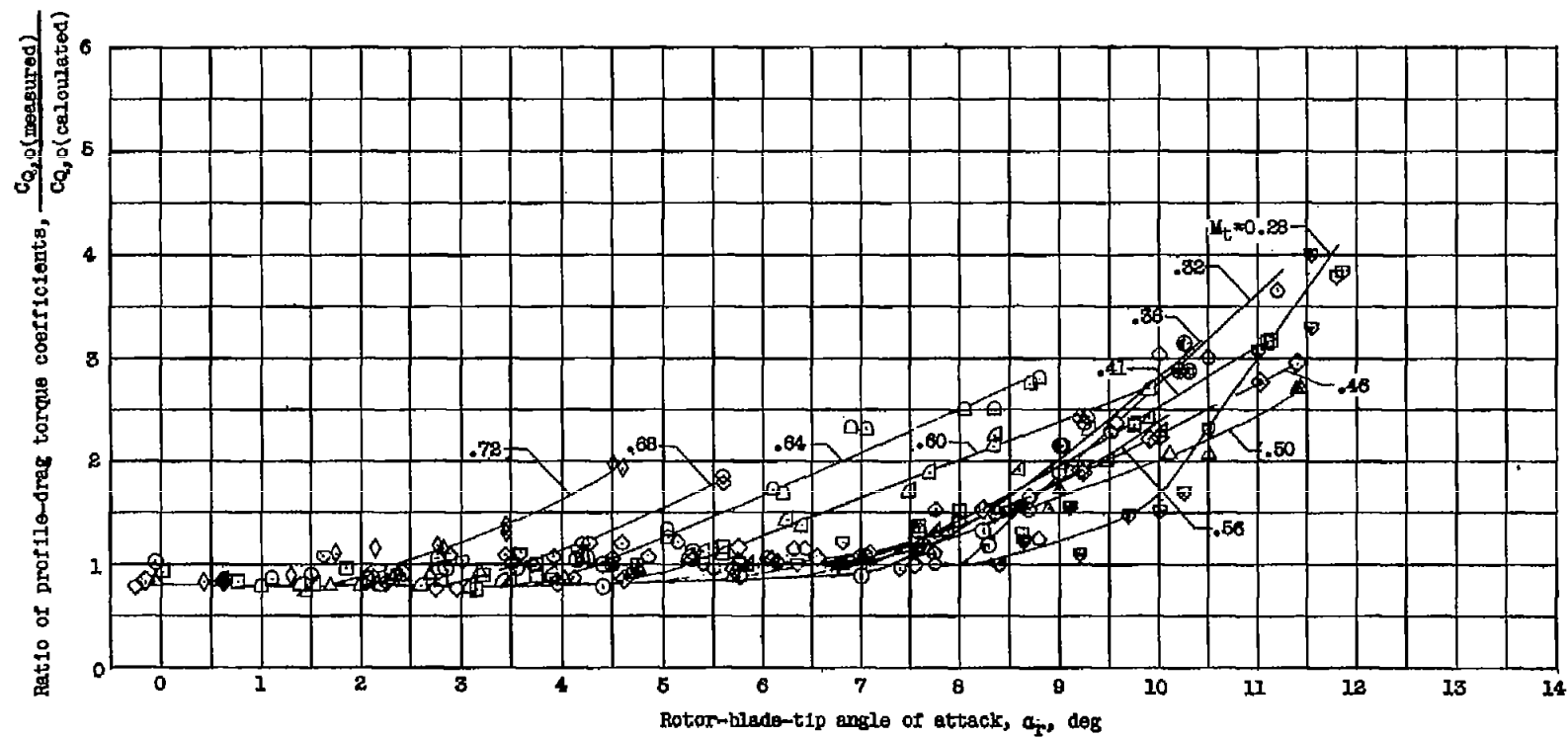
Figure 9.- Effect of tip angle of attack and Mach number on profile-drag torque of the rotor blades.
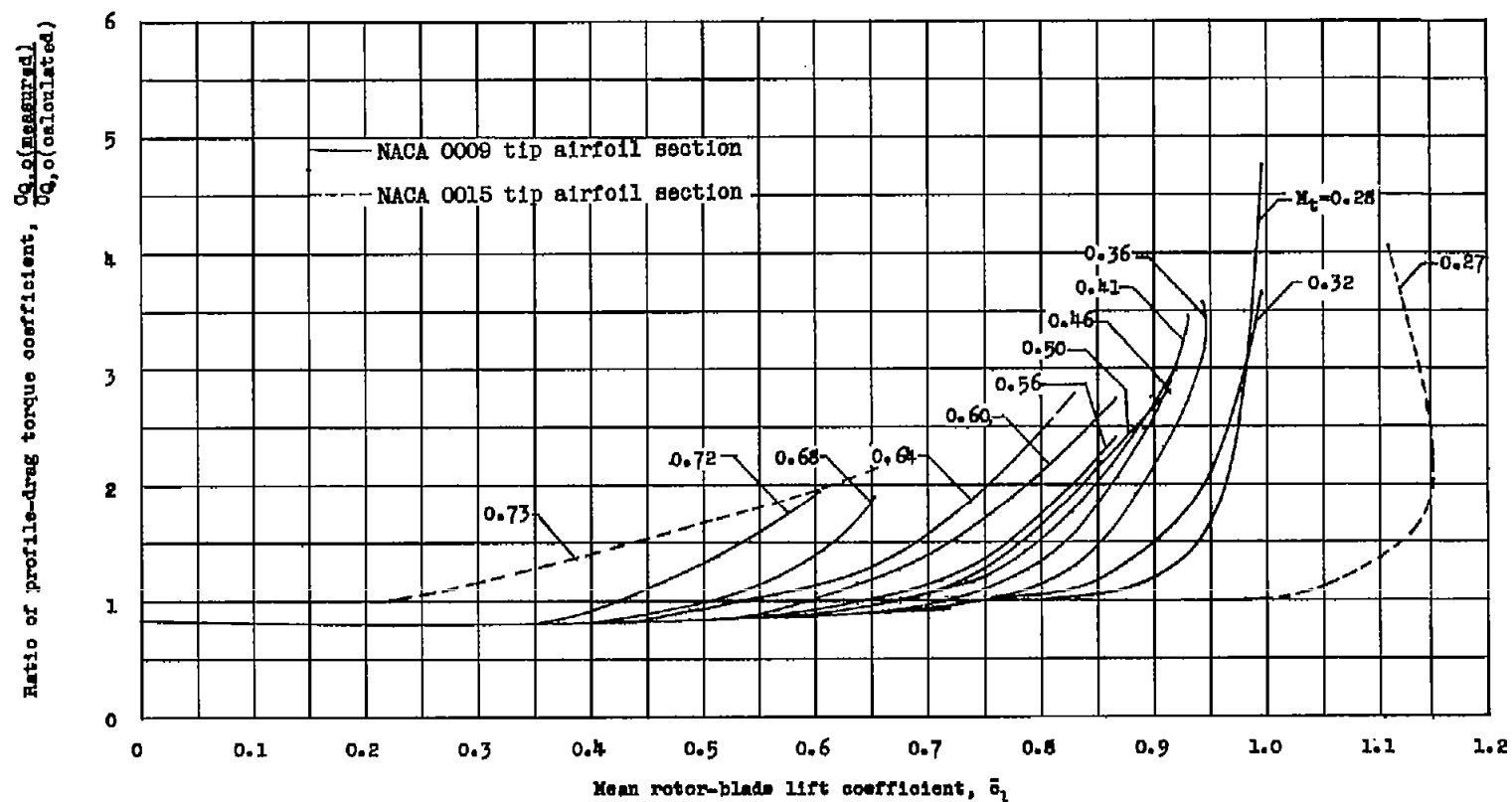
Figure 10.- Effect of rotor-blade mean lift coefficient and Mach number on profile-drag torque of rotor blades.
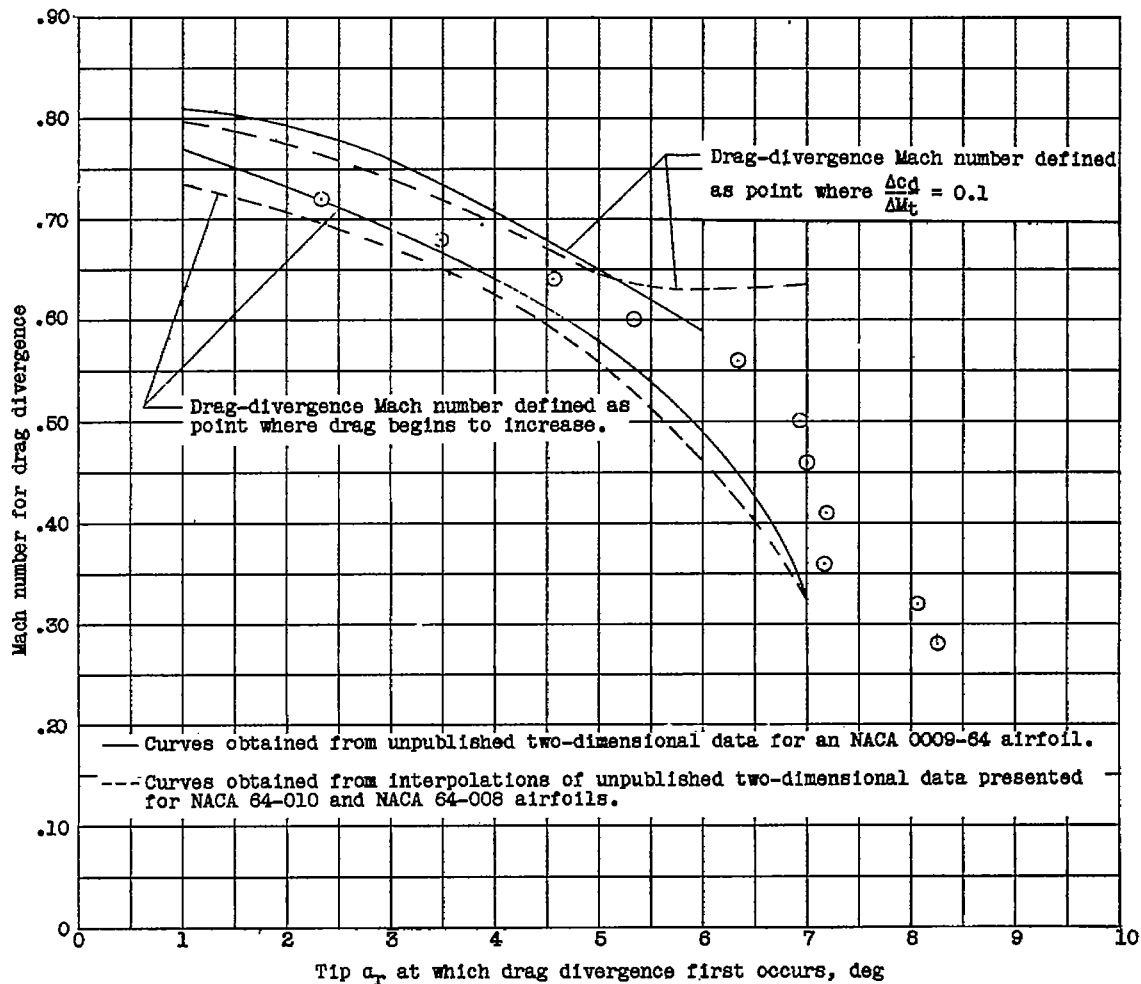
Figure 11.- Comparison of two-dimensional airfoil drag-divergence data
with the rotor experimental data. Symbols represent M_t and α_r
at which experimental data from the rotor blade separate from the
curve calculated by using the airfoil drag polar,

$$c_{d,o} = 0.0087 - 0.0216\alpha_r + 0.400\alpha_r{}^2.$$